

Preoperative to Intraoperative Space Registration for Management of Head Injuries

M. Gooroochurn, M. Ovinis, D. Kerr, K. Bouazza-Marouf, and M. Vloeberghs

Abstract—A registration framework for image-guided robotic surgery is proposed for three emergency neurosurgical procedures, namely Intracranial Pressure (ICP) Monitoring, External Ventricular Drainage (EVD) and evacuation of a Chronic Subdural Haematoma (CSDH). The registration paradigm uses CT and white light as modalities. This paper presents two simulation studies for a preliminary evaluation of the registration protocol: (1) The loci of the Target Registration Error (TRE) in the patient's axial, coronal and sagittal views were simulated based on a Fiducial Localisation Error (FLE) of 5 mm and (2) Simulation of the actual framework using projected views from a surface rendered CT model to represent white light images of the patient. Craniofacial features were employed as the registration basis to map the CT space onto the simulated intraoperative space. Photogrammetry experiments on an artificial skull were also performed to benchmark the results obtained from the second simulation. The results of both simulations show that the proposed protocol can provide a 5mm accuracy for these neurosurgical procedures.

Keywords—Image-guided Surgery, Multimodality Registration, Photogrammetry, Preoperative to Intraoperative Registration.

I. INTRODUCTION

THIS paper presents a registration framework designed to support image-guided solutions for three neurosurgical procedures that are routinely employed in the management of head injuries.

Registration is a general term used to describe the alignment of two datasets, with respect to a reference coordinate system, with the aim of reducing the disparity between them; alternatively recovering that disparity may be the goal. A registration basis consists of features chosen that relate both datasets in terms of the disparity involved. The datasets are then aligned by optimising a formulation of this registration basis. Image-to-patient registration basis can be broadly classified as either prospective or retrospective [1]. A common registration basis is point-based, with the majority of

frameless systems adopting this method for registration [2]. The gold standard in point-based registration is the use of surgically implanted fiducial markers. However, the use of this and other less invasive prospective techniques such as skin markers are not practical, because the need for surgery can usually only be established after a scan, not prior to it. Alternatively, anatomical features may be used [3]. Common anatomical features chosen for the head include the tragus, medial canthus, lateral canthus and nasion [3,4]. The use of anatomical features as a registration basis is appealing because of its retrospective nature. Intraoperatively, the required features for registration may be located through relatively inexpensive stereo white light imaging as long as the accuracy obtained is found to be satisfactory for the targeted procedures.

One of the earliest implementations of CT/MRI image-to-patient registration using stereo imaging was by [5]. A surface model of the patient, reconstructed intraoperatively using a stereo video system, was matched to a surface derived from CT/MRI. Patterned light was projected onto the patient to facilitate the stereo reconstruction. [6] used a laser scanner instead of a stereo video system to generate a surface model of the patient's face. The disadvantage of these techniques is that they require the use of specialised hardware such as 3D laser scanners or structured lighting. Additionally, surface matching is computationally intensive, as there is no closed form solution.

[7] used an alignment by mutual information approach described by [8] to register CT images to multiple video images. They observed that there is a mutual dependence between the image intensity of an object and the surface normal of a CT rendered model of the same object. The mutual dependence of information between the two modalities is used to undertake registration by maximising mutual information.

[9] developed a technique to register two or more video images of the human face to a 3D surface model using a similarity measure based on photo consistency. In photo consistency, an unknown surface can be reconstructed from a set of optical images by exploiting the consistency of intensities of points in each image. Conversely, given an accurately defined surface, photo consistency might be used as a measure of alignment of a surface to these optical images. The technique produced a 3D error of between 1.45 and 1.59 mm when the initial mis-registration was up to 16 mm/degree. As these methods are based on intensity rather than features,

The first four authors are from the Wolfson School of Mechanical and Manufacturing Engineering, Loughborough University, LE11 3TU, Loughborough, UK.

M. Gooroochurn and M. Ovinis are research students (e-mail: M.Gooroochurn@lboro.ac.uk and M.Ovinis2@lboro.ac.uk respectively).

D. Kerr and K. Bouazza-Marouf are senior lecturers (e-mail: d.kerr@lboro.ac.uk and k.bouazza-marouf@lboro.ac.uk respectively).

Prof. M. Vloeberghs is a consultant neurosurgeon at the Queen's Medical Centre, Nottingham University, NG7 2UH, Nottingham, UK (e-mail: Michael.Vloeberghs@Nottingham.ac.uk).

feature extraction or segmentation is not required. These techniques are therefore suited in applications where features cannot be reliably extracted. However, all these techniques require that the surfaces to be matched be roughly aligned, therefore limiting their application as a standalone registration method; a gross registration method is needed to first align the modalities roughly when a large difference in pose exists.

The three neurosurgical procedures for which our registration technique is developed pertain to emergency medicine. To this end, the protocol has been designed using machine vision tools to provide treatment as fast as possible within the accuracy limits allowed. While many registration techniques exist to perform preoperative to intraoperative registration, the majority require a combination of prior implantation of fiducial markers, costly intraoperative equipment such as optical trackers and 3D scanners, or additional radiation exposure inside the Operating Room (OR) e.g. with X-Ray Fluoroscopy. These factors would complicate and lengthen the targeted procedures, make them costly to implement and preclude their widespread application. It is a well-known fact that the medical community struggles to cope with such head trauma situations, especially due to the travelling time spent in reaching the appropriate medical premises that have the needed neurosurgical facilities. A simpler registration method can enable the application of image-guided solutions in conventional medical set-ups.

Since the targeted anatomy is the head, rigid registration between salient features in the CT surface rendered model and the corresponding features found on the patient's head in the OR is deemed adequate. Moreover, relying on the way neurosurgeons find the entry point for these procedures implies that a very high accuracy is not needed, unlike applications such as deep brain surgery and stimulation where sub-millimetre accuracy is usually a requirement. The entry point for ICP/EVD is normally found by offsetting two fingers width lateral to the sagittal suture and two fingers width anterior to the coronal suture on the non-dominant brain side of the head. Hence a 5mm accuracy is considered sufficient for these two procedures. As for CSDH, the entry point specified by the neurosurgeon can be offset by 5mm as well without any detrimental effect on the outcome of draining a large/medium traumatic haematoma capsule.

For the registration paradigm developed here, the preoperative space is characterised by a 3D CT surface rendered model of the patient's head, whereas the intraoperative space is built up from stereo camera views using Photogrammetry. Craniofacial landmarks, which can be found and paired in both modalities act as registration basis. The use of craniofacial landmarks instead of implanted fiducials means that no additional surgery is required. Stereo views of these extracted landmarks in white light modality allow their 3D reconstruction and ultimately registration with the preoperative space with no added exposure to radiation. The resulting transformation is then used to map the entry and target points specified by a neurosurgeon onto the patient's head inside the OR.

II. PROPOSED METHOD

A. Craniofacial Landmarks Selection

The ultimate aim of the registration is to map points found over the head surface (entry point) and inside the head (target point) from the CT space onto the patient's physical space in the OR. The craniofacial landmarks chosen as the registration basis should be visible and consistently reproducible in the CT model and corresponding landmarks need to be found in white light images as well. Their saliency is an important factor for the success of automated extraction, which is another aspect of the protocol currently looked at. Moreover these features should be widely spread, preferably close to or surrounding the points (entry and target points) to be mapped.

Choosing landmarks which are either close to or encompassing the entry and target points guarantees accurate interpolation using the transformation obtained from the registration. Unfortunately even shaving a patient's hair does not show up any salient natural landmarks on the patient's scalp whereas white light imaging precludes the use of any internal features. However, the head being a rigid body makes it a fair hypothesis that any set of points on the head that can be found robustly and paired between the two modalities can be used, provided they are not collinear and do not cover a minimal volume compared to the head volume. Registration based on facial features solely does not guarantee good accuracy as they cover only a small frontal volume of the head. Furthermore, routine CT scans are usually taken from the base to the vertex of the skull, thus preventing the use of nose and mouth features. In view of the above limitations, the ear tragus and the outer eye corners were chosen as natural landmarks for our registration process.

B. Simulated Target Registration for Selected Basis

It is useful to obtain error estimates for transforming given points on the surface of the head from one coordinate space to another using a given registration basis. The simulation presented next is the first of two simulations carried out to assess the adequacy of using the ear tragus and the outer eye corners for the registration task at hand. In general there are three types of registration errors: fiducial localisation error (FLE), fiducial registration error (FRE) and target registration error (TRE). FLE is defined as the distance between the measured and true position of a fiducial while FRE is the distance between the fiducial and its corresponding position after registration, with a fiducial being defined as an artificial point of reference for registration, usually attached to the patient's head. TRE is defined as the distance between the expected location of a desired anatomical target and its actual location. For a rigid-body point-based registration, the 3D relationship between FLE and TRE [10] is:

$$TRE^2 = \frac{FLE^2}{N} \left(1 + \frac{1}{3} \sum_{k=1}^3 \frac{d_k^2}{f_k^2} \right) \quad (1)$$

where d_k is the distance of the targets from the k^{th} principal

axis of the landmark configuration, k is the number of dimensions and f_k is the RMS distance of the fiducials from the k^{th} principal axis. As will be shown later, our method proposes a marker-less registration system using natural anatomical landmarks in place of fiducials. The possible TREs using the proposed registration basis have been simulated using Equation 1 for landmark localisation errors of 5mm in both imaging modalities. This 5mm value has no direct bearing on the overall 5mm target location accuracy aimed at; it is instead based on experience with manual extraction of the landmarks. This simulation, shown in Fig. 1, allows us to visualise contours of TRE error for the chosen 5mm FLE error for the coronal, sagittal and axial views.

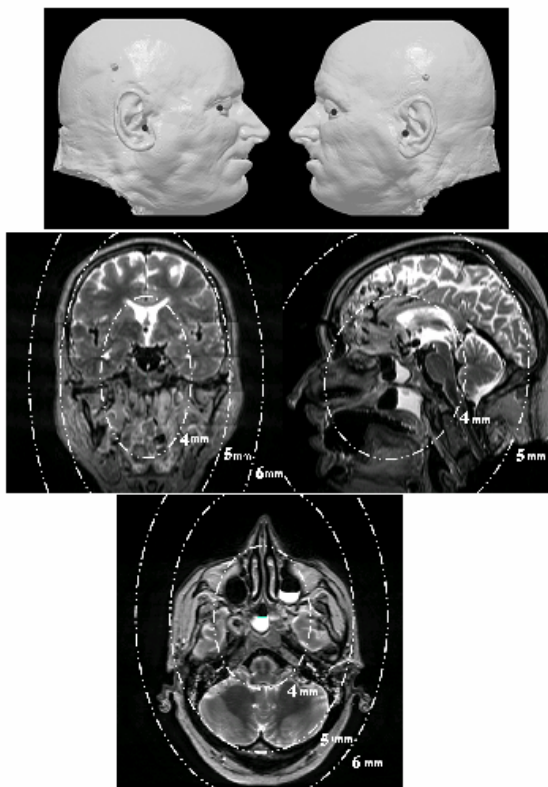


Fig. 1 Anatomical landmarks used and corresponding TRE contours for a FLE of 5mm¹

As can be seen, the head is almost totally enclosed by the 5mm TRE contour, showing the desired overall error is achievable with FLEs of this magnitude.

C. Registration Protocol

The intraoperative component of the registration framework can be classified as pose estimation and 3D head modelling. In [11], Ansari et al. use a camera set-up with two views (frontal and profile) to reconstruct the 3D coordinates of facial features. The facial features found on the hidden side of the face with respect to the profile view are reconstructed based

on face symmetry. The proposed registration technique uses the ear tragus as a feature, which does not appear in a frontal view. So an additional intermediate view, between the frontal and profile view is required. This will enable the reconstruction of the two outer and inner eye corners for each eye and one ear tragus fully, and with these five points, rigid-body point-based registration would be feasible. A schematic of the three camera system as shown in Fig. 2(a) can be used for this purpose.

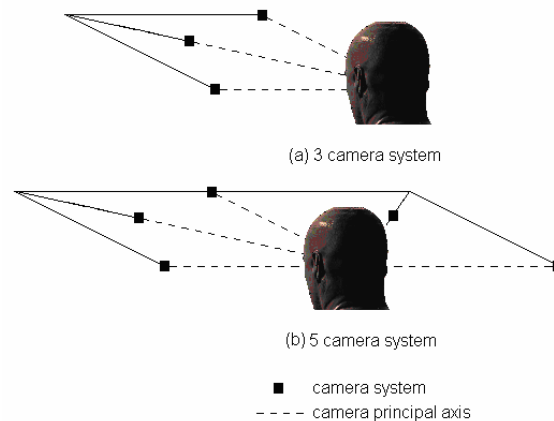


Fig. 2 Schematic of Camera System

However, for the preliminary investigation presented, the full 5 camera set-up shown in Fig. 2(b) has been used. The protocol could not be tested on real data as a common dataset in both modalities for a given person was not available due to the cost and complexity of arranging clinical trials. Hence the points extracted and reconstructed are not based on symmetry of the face, but are all coordinates reconstructed by direct application of Photogrammetry on corresponding point pairs.

The selected craniofacial landmarks are intuitive and straightforward for a non-expert operator to pick with a fair degree of accuracy. For the investigation illustrated in this paper, the features have been manually selected from the 3D model and the projected views. Automated methods of extraction are being developed in parallel aimed at providing an automated registration solution to the user which he/she then validates by visual inspection.

Fig. 3 shows the projected frontal, profile and intermediate views obtained from a CT head model based on the 5 camera system set-up. Marking the craniofacial features shown in these views and pairing them offer the possibility to reconstruct their 3D coordinates using Photogrammetry techniques, provided the views have been calibrated. The simple Direct Linear Transformation (DLT) method without error correction [12] has been used throughout the testing of the proposed method for calibrating the views and reconstructing 3D coordinates as it is deemed sufficiently accurate for the targeted 5mm accuracy. Section III uses such simulated views from CT models to generate a frontal, two intermediate and two profile views for fifteen independent CT datasets.

¹ [CT/MRI data from US National Library of Medicine's Visible Human Project®]

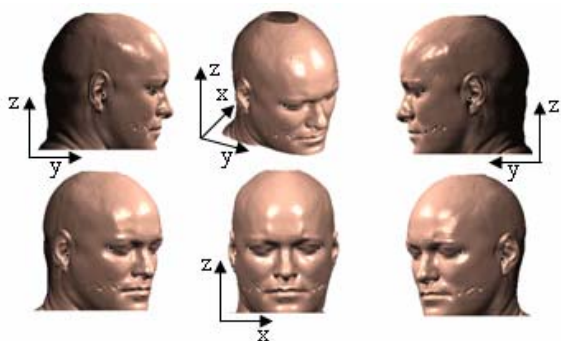


Fig. 3 Projected Head Views²

Performing reconstruction from stereo views necessitates calibrated camera systems; it is recommended to calibrate the space so that the object to be reconstructed lies within the calibrated volume as extrapolation outside that space can lead to erroneous results [13]. Hence any image captured should be delimited to fall within the field of view in each camera corresponding to that occupied during calibration. A calibration object encompassing the human head has been designed for this purpose.

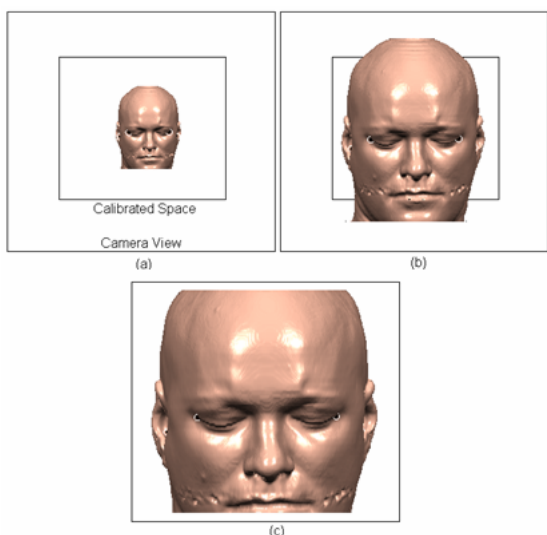


Fig. 4 Fitting Image in Calibrated Region³

Fig. 4 shows three possible scenarios of coverage for the field of view of the camera with respect to the calibrated space in the frontal view. Case (b) has an adequate coverage in the frontal view as the face area closely fills the field of view corresponding to the calibrated space. Assuming that the human head does not vary widely over the general population, the set-up of the cameras necessarily implies correct positioning in the other views as well. Under these assumptions, cases (a) and (c) are definitely out of the correct

space and would lead to extrapolation outside of the calibrated volume. The variability in the size of the human head means that the field of view cannot always be optimally filled in both the frontal and profile views. This variability has been considered in the design of the calibration object by choosing the dimensions so that it covers any human head size.

The placement of the camera system so as to fill the calibrated space adequately is planned in the frontal and profile views. The extreme position for the boundary of the calibrated space is made to match with the nose in the profile image by having a vertical datum line (overlaid on a live TV image of the patient) for the user to approximately align the nose tip to. This ensures that the patient is properly placed with respect to the frontal view in terms of the camera working distance. Additionally, having a central vertical line in the frontal view, which is aligned with the patient's nose centre and the middle of the two eyes, locates the patient correctly in the profile view. An additional horizontal line in the frontal view which is aligned to the eye corners sets the patient's head location with respect to the vertical axis of the camera image planes. Fig. 5 illustrates these datum lines in the frontal and profile views.



Fig. 5 Datum Lines for Initial Camera Set-up

Finally, graduations are provided on the horizontal datum line in the frontal view, which is to be aligned with the eye corners. By using these graduations, the user can place the frontal camera so that the distance of each corresponding eye corner (left inner eye corner to right inner eye corner or left outer eye corner to right outer eye corner) to the vertical datum line is more or less equal. This compensates for excessive yaw of the head and ensures that a frontal or near frontal view is obtained.

III. METHODOLOGY FOR PRELIMINARY VALIDATION

A. Craniofacial Feature Reconstruction

This section describes the work undertaken for reconstructing points marked on an artificial human male skull. Fig. 6 shows the 22 points used ranging from A to V (A is not visible as it lies on the top). To provide a calibrated space for the Photogrammetry tests and subsequently for the registration framework, a calibration object was designed which encompassed the volume of the human head. Its dimensions were 200mm x 300mm x 300mm. A calibration bar was manufactured which could accommodate any one of the calibration object and the skull at a time, thus providing a

² CT slices have been taken from the patient contributed image repository at <http://www.pcir.org>

³ CT slices have been taken from the patient contributed image repository at <http://www.pcir.org>

common frame of reference for the skull and the calibration object.



Fig. 6 Locus of Points marked over the Skull

During accuracy validation experiments, stereo views of the calibration object and the skull were taken in turn. The origin of the calibration bar was used as the (X,Y,Z) World Coordinate System (WCS). The simple DLT technique was used for calibrating the cameras and reconstructing points over the skull with respect to the WCS. With the reference coordinates known with respect to the WCS via prior Coordinate Measuring Machine (CMM) measurements, the errors due to photogrammetry can be computed. Errors in world coordinates (X,Y,Z) are recorded in Table I for a general camera configuration viewing the front of the skull. Only points which appeared in both stereo views and those found in the upper region of the face have been reconstructed.

The highest RMS error obtained was 1.57mm for point N while the highest error along the individual dimensions was 1.99mm for point T along the z-direction. These Photogrammetry results provide a good basis for comparison to the corresponding ones obtained in the simulation study presented later.

TABLE I
PHOTOGRAMMETRY ERRORS FROM SKULL POINTS RECONSTRUCTION

Skull Points	X (mm)	Y (mm)	Z (mm)	RMS error (mm)
F	0.62	0.53	1.84	1.16
G	-0.16	-0.34	1.94	1.14
L	0.53	-0.05	1.40	0.87
M	0.90	-0.31	1.22	0.90

N	0.68	1.82	1.91	1.57
P	0.72	-0.18	1.90	1.18
R	0.08	0.68	1.95	1.19
T	0.37	0.68	1.99	1.23

The simulation also performs registration of the CT space and the reconstructed projected space using the coordinates of the landmarks as the registration basis. In performing such a registration, the coordinates in the CT model are considered as reference coordinates. A similar exercise can be done for the skull as well. While the results obtained for the Photogrammetry in the simulation study are just representations of what might be expected in practice, tests with the skull yield error estimates on real data for the Photogrammetry. On the other hand, the skull does not represent the actual landmarks that will be reconstructed as bone data are used instead of skin information. The latter is however used during the simulation study with projected views from the surface rendered CT model. The additional benefit of the simulation is that the registration framework can be validated over a wide set of data (15 head models).

In summary, the Photogrammetry results from the skull yield error estimates that would be expected in practice with the Machine Vision algorithms employed while the simulation study described in the next section is closer to the actual registration in the sense that it is applied on skin data and validates the protocol over a broader range of data. To provide a further basis for comparison, registration of the skull based on the reference and reconstructed coordinates is carried out next using points on the skull with similar distribution as the eye corner and ear tragus. Points L, N, D and I are such points corresponding to the eye corners and ear tragus respectively. Two experiments were undertaken, with camera configurations viewing the right side of the skull to yield reconstructions for points L and D and the left side of the skull to allow reconstructions for points N and I.

Table II and Table III present the photogrammetric error estimates obtained for these four points. These points were used to perform the registration and point A, located on the top of the cranium in the skull was mapped from the original reference space to the reconstructed space. The following error was obtained in the three dimensions of the WCS: [-0.61mm, -1.40mm, 0.74mm] with an RMS error of 0.98mm. The next section presents the simulation study using surface rendered CT models and projected views for similar tests performed on the skull.

TABLE II
PHOTOGRAMMETRY ON RIGHT SIDE OF SKULL

Skull Points	X (mm)	Y (mm)	Z (mm)	RMS error (mm)
L	-0.30	-0.08	1.70	1.00
N	-	-	-	-
D	-0.07	-0.69	0.59	0.52
I	-	-	-	-

TABLE III
PHOTOGRAMMETRY ON LEFT SIDE OF SKULL

Skull Points	X (mm)	Y (mm)	Z (mm)	RMS error (mm)
L	-	-	-	-
N	-0.11	-0.95	2.05	1.31
D	-	-	-	-
I	-0.34	-0.11	1.37	0.82

B. Projection Views Generation and Processing

As pointed out earlier, the unavailability of a common set of CT and white light images for a range of human subjects has precluded the testing of the system on a real dataset so far. This is due to the complexity of the procedure for undertaking clinical trials and the associated high costs. So the results presented in this section are simulated ones. However, it is believed that these estimated coordinates of the manually extracted features represents the typical errors involved in reconstructing the actual features in practice. Additionally, tests on the skull presented in section A can be used as a yardstick to assess the validity of the Photogrammetry process in isolation, if necessary.

The 3D surface rendered models were created from CT datasets from various sources such as the US National Library of Medicine (Visible Human Project), the Patient Contributed Image Repository⁴, the Association of Electrical and Medical Imaging Equipment Manufacturers⁵, and numerous databases available in the public domain containing DICOM compliant CT images⁶ as well as from anonymised CT images of patients. The head CT scans used in the surface reconstruction were 512 x 512 x 1 voxels with slice thicknesses of 0.4 - 1.25 mm. The surface reconstruction of these DICOM compliant scans was performed by using an implementation of an isosurface algorithm to construct a 3D surface rendering.

The five views are projected from the 3D CT model at azimuth angles of 0, 45, 90, -45 and -90 degrees corresponding to the frontal, left intermediate, left profile, right intermediate and right profile images respectively. These projected views are marked with control points whose 3D coordinates are known in the CT model and appear on the projected views. This enables calibration of the different views; the simple DLT approach has been used for this purpose. The craniofacial landmarks to be extracted and reconstructed thereafter are not used as part of the calibration control points. From the DLT parameters recovered, the selected craniofacial landmarks are manually picked in stereo views and used for reconstructing the landmarks' 3D coordinates. Clearly, only the intermediate and profile views suffice and have been used for tests on the 15 head models. For these Photogrammetric reconstructions, the maximum RMS error obtained was 1.04mm for the left ear corresponding to model 1. The maximum error in the three

dimensions was 1.28mm in the x-direction corresponding to model 2 for the left ear.

For registration of the CT model and the simulated white light modality based on the craniofacial features, it is expected to have identity for the rotation matrix and zero for the translation vector due to the same pose of the model in both datasets. Any divergence from this ideal result is due to the errors in reconstructing the features in the white light modality. The next calculation performed was to register the two datasets using the coordinates of the features from the CT model and the reconstructed ones from Photogrammetry. This serves to validate how well the estimated features correspond and contribute to the overall error after registration. Four arbitrary points (Fig. 7) were picked over the face and mapped from the CT space onto the reconstructed coordinate system. Table IV shows the results for the 15 head models.

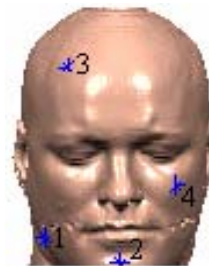


Fig. 7 Arbitrary points selected for mapping⁷

TABLE IV
REGISTRATION ERRORS FROM SIMULATED TESTS

Model	RMS Error (mm)			
	Point no. (in Figure 7)			
	1	2	3	4
1	0.52	0.46	0.42	0.52
2	0.47	0.24	0.46	0.41
3	0.26	0.28	0.21	0.32
4	0.39	0.28	0.38	0.26
5	0.36	0.33	0.35	0.29
6	0.48	0.38	0.68	0.35
7	0.20	0.36	0.35	0.31
8	0.50	0.40	0.32	0.32
9	0.43	0.50	0.59	0.54
10	0.16	0.22	0.16	0.26
11	0.49	0.27	0.31	0.25
12	0.38	0.43	0.51	0.34
13	0.21	0.32	0.36	0.35
14	0.19	0.30	0.21	0.35
15	0.18	0.43	0.41	0.39

C. Simulating the Procedure

This section aims at replicating the protocol followed in a normal surgery scenario with the selection of entry and target points by the neurosurgeon (Fig. 8).

⁷ CT slices have been taken from the patient contributed image repository at <http://www.pcir.org>

⁴ <http://pcir.org>

⁵ <ftp://medical.nema.org/MEDICAL/Dicom/Multiframe>

⁶ <http://apps.sourceforge.net/mediawiki/gdcm>

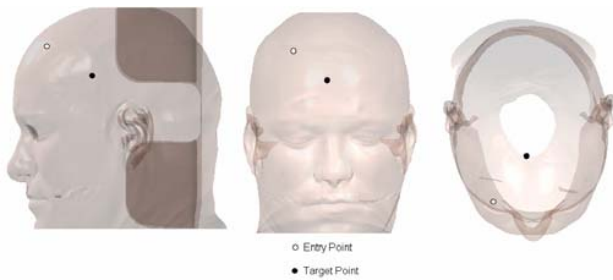


Fig. 8 Entry and Target Points for Model 1⁸

These are done on given CT scans which can then be located on the patient. The registration transformation obtained earlier is used to map these points onto the reconstructed coordinate system. A spherical representation of the trajectory vector provides the length of the trajectory and its orientation in space. These metrics are computed in each coordinate system as a means to assess accuracy, with ϕ being the angle from the z-axis and θ the angle in the x-y plane from the x-axis. For the fifteen head models, the maximum error for ϕ was 0.25° for which θ equals 0.23° while the maximum value for θ was 0.44° with an associated value of 0.07° for ϕ .

IV. DISCUSSION

The methodology employed for validating the proposed registration technique is two-fold. Using the analytical expression given by Fitzpatrick et al. [10], the loci of Target Registration Errors for a Fiducial Localisation Error of 5mm over the chosen registration basis has been simulated. With a targeted accuracy of 5mm, the entry and target points have been found to lie within the 5mm contour. This shows that the distribution of the ear tragus and eye corner is spread out sufficiently so that as long as a 5mm accuracy is achieved in extracting the craniofacial features, the overall registration accuracy will satisfy the requirements for the three neurosurgical procedures.

The second simulation study aimed at replicating the proposed registration paradigm by using projected views of 3D CT models to represent white light stereo views. Due to the unavailability of a common dataset in the CT and white light modalities, a method was adopted to illustrate the registration procedure while providing error estimates. The extent to which the generated surface approximates the true skin depths at different points on the head can be validated only by running the protocol on real patient data. However, previous research supports the use of CT generated skin depth as a good approximation to real tissue depth [14-18]. Kim et al. [18] did a study on the measurement accuracy using CT under different scanning protocols. In particular, they looked at the accuracy of facial soft tissue thickness measurements in multiplanar reconstructed CT images using various slice

thickness (0.5 – 7 mm), pitch (1:1 – 2:1), and types of scanner (conventional, spiral, multidetector). They found mean deviation to be within 0.43 mm in all instances when compared to actual physical measurements.

Control points were used over the head model to calibrate the projected views and ultimately the 3D coordinates of the craniofacial landmarks were reconstructed from the calibrated stereo views. The Photogrammetric errors incurred in using such an approach are representative of what is expected by using a calibration object, which is the normal practice as part of the proposed registration technique. Experimental work using an artificial skull gave error estimates comparable to those obtained in the simulation study. Specifically, the maximum RMS error for the artificial skull was found to be 1.57mm while the simulation analysis yielded a maximum RMS error of 1.04mm. The smaller error in the latter may be attributed to non-correction of radial and decentring distortions in the DLT algorithm which were present in the camera images of the skull and non-existent in the projected views from the CT head model.

The use of the selected landmarks as a basis for registration shows that rigid registration can be used to map the chosen entry and target points for the set accuracy. This has been validated both for the experimental work on the skull and the simulation study with head models. For the simulation, registration RMS errors of less than 1mm were obtained for points selected around the face while case studies involving the selection of entry and target points on the different head models showed acceptable angular deviation from the original set trajectory when mapped into a spherical representation. Similar registration and mapping with the skull gave an overall RMS registration error of about 1mm.

The simulation results are based on manual selection of the craniofacial landmarks in the two modalities and show good correspondence to the errors incurred in the experimental work related to the Photogrammetry of the skull. Hence the results of the simulation can be extended to make practical deductions of expected errors in the actual protocol. With the error obtained for the maximum RMS registration error (0.68mm) almost an order of magnitude less than the targeted accuracy (5mm), the further errors introduced in the system during actual operation in extracting the craniofacial features in the two modalities are likely to still yield an error less than 5mm. This hypothesis is based on the assumption that the variability in extracting the features or validating the correctness of their extraction will not be significantly different from the subjective extraction of these landmarks during the simulation study carried out. Therefore the overall registration error is expected not to exceed the targeted 5mm. An actual implementation of the registration protocol will provide definite measures of the adequacy of the proposed approach.

V. CONCLUSION

A registration protocol for preoperative CT to

⁸ CT slices have been taken from the patient contributed image repository at <http://www.pcir.org>

intraoperative white light images has been described. Specifically, the proposed registration has been devised in view of supporting three neurosurgical procedures that are emergency in nature. Simulation of the registration framework gave errors almost an order of magnitude less than the required accuracy to undertake these procedures while simulation of the loci of TRE for an FLE of 5mm gave isocontours that predict acceptable errors for the target and entry points normally employed in the neurosurgical procedures. Experimental results show similar error estimates as those obtained through the simulation study. The similarity between the feature extraction/validation methods in the actual protocol and that simulated makes it reasonable to assume errors less than 5mm will be obtained when the protocol is implemented. Definitive results will however be obtained to support this claim through experimental work on a common set of CT and white light images. A methodology based on datum lines marked on the displays showing the frontal and profile views has been formulated for placing the camera system with respect to the patient so that the latter lies in the calibrated space. The next step will be to implement the registration protocol on real datasets in both modalities. Machine vision tools will also be introduced into the registration framework to help in localising and extracting craniofacial features in the CT and white light modalities thereby reducing subjectivity in the process. The proposed registration method can also be used as part of other registration methods where gross alignment is first needed.

REFERENCES

- [1] J.M. Fitzpatrick, D. L. G. Hill and C. R. Maurer Jr, "Image registration", in *Handbook of Medical Imaging II: Medical Image Processing and Analysis*, vol. 2, M. Sonka and J. M. Fitzpatrick, Eds. Bellingham, WA: SPIE Press, 2000, pp. 447-513.
- [2] J. McInerney and D. W. Roberts, "Frameless stereotaxy of the brain," *Mt. Sinai J. Med.*, vol. 67, Sep. 2000, pp. 300-310.
- [3] C. R. Maurer, R. P. Gaston, D. L. G. Hill, M. J. Gleeson, M. G. Taylor, M. R. Fenlon et al., "AcouStick: A Tracked A-Mode Ultrasonography System for Registration in Image-Guided Surgery," *LECTURE NOTES IN COMPUTER SCIENCE*, 1999, pp. 953-962.
- [4] M.J. Citardi, "Computer-aided frontal sinus surgery", *Otolaryngol. Clin. North Am.*, vol. 34, 2001, pp. 111-122.
- [5] A.C. Colchester, J. Zhao, K. S. Holton-Tainter, C. J. Henri, N. Maitland, P. T. Roberts et al., "Development and preliminary evaluation of VISLAN, a surgical planning and guidance system using intra-operative video imaging", *Med. Image Anal.*, vol. 1, Mar. 1996, pp. 73-90.
- [6] W. E. L. Grimson, G. J. Ettinger, S. J. White, T. Lozano-Perez, W. M. Wells III and R. Kikinis, "An automatic registration method for frameless stereotaxy, image guided surgery, and enhanced reality visualization", *Medical Imaging, IEEE Transactions on*, vol. 15, 1996, pp. 129-140.
- [7] M.J. Clarkson, D. Rueckert, D. L. G. Hill and D. J. Hawkes, "Using photo-consistency to register 2D optical images of the human face to a 3D surface model", *IEEE Trans. Pattern Anal. Mach. Intell.*, vol. 23, 2001, pp. 1266-1280.
- [8] P. Viola and W.M. Wells III, "Alignment by Maximization of Mutual Information", *International Journal of Computer Vision*, vol. 24, 1997, pp. 137-154.
- [9] M.J. Clarkson, D. Rueckert, D.L. Hill and D. J. Hawkes, "Registration of multiple video images to preoperative CT for image-guided surgery", *Proceedings of SPIE*, vol. 3661, 2003, pp. 14-23.
- [10] J.M. Fitzpatrick, J.B. West and C.R. Maurer Jr, "Predicting error in rigid-body point-based registration", *Medical Imaging, IEEE Transactions*, vol. 17, 1998, pp. 694-702.
- [11] A-Nasser Ansari and Mohamed Abdel-Mottaleb, "Automatic facial feature extraction and 3D face modelling using two orthogonal views with application to 3D face recognition", *Pattern Recognition* vol. 38 (12), Dec 2005, pp 2549-2563.
- [12] Y.I. Abdel-Aziz. and H.M. Karara, "Direct linear transformation from comparator coordinates into object space coordinates in close-range photogrammetry." *Proceedings of the Symposium on Close-Range Photogrammetry*, Falls Church, VA: American Society of Photogrammetry, 1971, pp. 1-18.
- [13] LIANG CHEN, C.W. ARMSTRONG and D.D. RAFTOPOULOS, "An investigation on the accuracy of three-dimensional space reconstruction using the direct linear transformation technique", *Journal of biomechanics*, Vol. 27, No. 4, 1994, pp. 493-500,
- [14] M.G.P. Cavalcanti, S.S. Rocha and M.W. Vannier, "Craniofacial measurements based on 3D-CT volume rendering: implications for clinical applications", *Dentomaxillofacial Radiology*, vol. 33, 2004, pp. 170-176.
- [15] D.X. Liu, C.L. Wang, L. Liu, Z.Y. Dong, H.F. Ke and Z.Y. Yu, "The accuracy of 3D-CT volume rendering for craniofacial linear measurements", *Shanghai Kou Qiang Yi Xue*, vol. 15, Oct. 2006., pp. 517-520.
- [16] K. Kim, A. Ruprecht, G. Wang, J. Lee, D. Dawson and M. Vannier, "Accuracy of facial soft tissue thickness measurements in personal computer-based multiplanar reconstructed computed tomographic images", *Forensic Sci. Int.*, vol. 155, Dec 1. 2005, pp. 28-34.
- [17] A.A. Waitzman, J.C. Posnick, D.C. Armstrong and G.E. Pron, "Craniofacial skeletal measurements based on computed tomography: Part I. Accuracy and reproducibility", *Cleft Palate. Craniofac. J.*, vol. 29, Mar. 1992, pp. 112-117.
- [18] K. Togashi, H. Kitaura, K. Yonetsu, N. Yoshida and T. Nakamura, "Three-Dimensional Cephalometry Using Helical Computer Tomography: Measurement Error Caused by Head Inclination", *Angle Orthod.*, vol. 72, 2002, pp. 513-520.